# Calculation of the Lattice Specific Heat of Very Dilute Al:Ag Alloys

M. D. Tiwari, K. M. Kesharwani, and Bal K. Agrawal
*Department of Physics, University of Allahabad, Allahabad-2, India*
(Received 1 June 1972)

A detailed study of the effects of force-constant changes due to impurity atoms on the lattice specific heat has been made in very dilute aluminum-silver alloys. Numerical computations have been performed for $Al_{99.50}Ag_{0.50}$ and $Al_{99.05}Ag_{0.95}$ alloys. Almost all of the of the contribution to the specific heat arises because of $F_{1u}$ resonance modes and the contribution increases with increase in temperature. A very good agreement between the theory and the experiment has been observed in both the alloys. The use of an effective force constant which has been defined earlier is found to be very appropriate in making simple calculations for the specific heat. The observed discrepencies between the results obtained in the frame work of effective force constant and those obtained in a realistic manner are seen to be less than 12% at very low temperatures and are even smaller at comparatively higher temperatures.

## I. INTRODUCTION

The doping of a crystal with defects changes the vibrational properties of the pure crystal.[1-3] There are alterations in the frequencies of the normal modes of vibrations of the crystal lattice and in the pattern of the atomic displacements in the normal modes. Localized modes can appear activated by a light impurity or by a defect coupled to its neighboring atoms more strongly than to a host atom. The frequencies of the localized or bound states lie in ranges forbidden for the normal modes of the pure-host crystal. Quasilocalized or resonance modes may also appear for a heavy impurity or a defect coupled weakly to its neighbors as compared to the host atom. The frequencies of the resonance modes lie in the ranges of the frequencies allowed to the normal modes of the pure-host crystal. These modes are characterized by a large vibrational amplitude of the defect or of those atoms with which it directly interacts. An increase in the density of states near the resonance frequency is observed which gives rise to resonance-type peaks in the frequency spectrum of the impure crystal. Further, these modes have finite lifetimes because they can decay into the band modes. An extensive study of the changes in the phonon spectrum due to small concentrations of very heavy or very light impurities has been made by performing inelastic-neutron-scattering experiments.[4-6]

The effects of the defects on the frequency spectrum of an imperfect crystal may be studied by measuring the lattice contribution to the specific heat. The contribution of localized modes to the lattice part of the low-temperature specific heat is too small to be detected in the experimental measurements. On the other hand, the contribution of the low-frequency resonance modes to low-temperature specific heat is appreciable and is accessible to observation. The possibility of occurrence of a substantial enhancement due to low-frequency resonance modes was suggested by Lehman and DeWames[7] and independently by Kagan and Iosilevskii.[8] This enhancement in the specific heat due to heavy impurities in metals has been reported in a number of papers.[9-11]

Very recently, Hartmann *et al.*[12] have measured the lattice part of the specific heat of aluminum containing low concentrations (0.50 and 0.95 at.%) of Ag at low temperatures and have shown that the mass-defect calculation accounts for about 80% of the observed change in the specific heat. In the present paper the effects of force-constant changes on the lattice specific heat have been studied in a crystal containing a low concentration of impurities. Numerical computations have been made for the two dilute alloys $Al_{99.05}Ag_{0.95}$ and $Al_{99.5}Ag_{0.5}$. A good agreement between the theory and the experiment has been observed.

A brief account of a low-concentration Green's-function theory for the change in the density of states and the calculation for the change in the lattice specific heat for an imperfect crystal is given in Secs. II A and II B, respectively. The localized-perturbation model for the defect is discussed in Sec. II C. The lattice dynamics and the calculation of Green's function for aluminum are discussed in Secs. III A and III B, respectively. The enhancement in the specific heat is determined and the results, based on an effective force constant, are obtained in Sec. III C and Sec. III D, respectively. These results are discussed and summarized in Sec. IV.

## II. THEORY

### A. Density of States in Imperfect Crystal

If $N_0(\omega^2)d\omega^2$ is the number of normal modes whose squared frequencies lie in the interval $(\omega^2, \omega^2+d\omega^2)$, in the limit as $d\omega^2$ tends to zero, then the density of states in a pure crystal is denoted by $N_0(\omega^2)$ and is expressed as

$$N_0(\omega^2)=\sum_{\vec{k},s}\delta(\omega^2_{\vec{k},s}-\omega^2)\ , \tag{1}$$

where $\omega_{\vec{k},s}$ is the phonon frequency corresponding to the wave vector $\vec{k}$ and the polarization branch $s$.

The time-independent equation of motion can be written

$$(\underline{L}_0-z\underline{I})\vec{\psi}_0=0\ , \tag{2}$$

with $\underline{L}_0=\underline{M}_0^{-1/2}$; $\underline{\phi}_0\underline{M}_0^{-1/2}$; $\underline{M}_0$ and $\underline{\phi}_0$ are the mass and the force-constant matrices of the perfect crystal, respectively. $\vec{\psi}_0$ is a vector which is related to the usual atomic displacement vector $\vec{u}$ by

$$\vec{u}=\underline{M}_0^{-1/2}\vec{\psi}_0\ . \tag{3}$$

Here $\underline{I}$ is the unit matrix and $z$ denotes complex squared frequency, given by

$z=\omega^2+2i\omega\xi$ in the limit $\xi\to 0$.

For a crystal containing a finite concentration of defects which have different masses and interactions with its neighbors, the time-independent equation of motion may be written

$$[\underline{L}_0+\underline{P}(\omega^2)]\vec{\psi}=\omega^2\vec{\psi}\ , \tag{4}$$

where $\underline{P}(\omega^2)$, the perturbation matrix caused by the defects, is explicitly given by

$$\underline{P}(\omega^2)=-\omega^2\underline{M}_0^{-1/2}\Delta\underline{M}\,\underline{M}_0^{-1/2}+\underline{M}_0^{-1/2}\Delta\underline{\phi}\,\underline{M}_0^{-1/2}\ . \tag{5}$$

Here the new mass and force-constant matrices of the imperfect crystal have been denoted by $\underline{M}_0+\Delta\underline{M}$ and $\underline{\phi}_0+\Delta\underline{\phi}$, respectively, and $\vec{\psi}$ is the corresponding vector of the lattice.

The Green's function for a perfect lattice is defined by

$$\underline{G}^0(z)=(\underline{L}_0-z\underline{I})^{-1}\ . \tag{6}$$

Equation (1) can be rewritten

$$N_0(\omega^2)=\frac{1}{\pi}\mathrm{Im}[\,\mathrm{Tr}(\underline{L}_0-z\underline{I})^{-1}]$$

$$=-\left(\frac{1}{\pi}\right)\mathrm{Im}\frac{d}{d\omega^2}(\ln|\underline{L}_0-z\underline{I}|)\ . \tag{7}$$

For an imperfect crystal we may similarly write for the density of states

$$N(\omega^2)=-\left(\frac{1}{\pi}\right)\mathrm{Im}\frac{d}{d\omega^2}(\ln|\underline{L}-z\underline{I}|)\ , \tag{8}$$

where $\underline{L}$ is the mass-reduced force constant matrix for the imperfect crystal.

Equation (8) can also be written

$$N(\omega^2)=-\left(\frac{1}{\pi}\right)\mathrm{Im}\frac{d}{d\omega^2}\{\ln[\,|\underline{I}+\underline{G}^0\underline{P}(\omega^2)|\,|\underline{L}_0-z\underline{I}|\,]\}\ . \tag{9}$$

The change in the density of states due to defects is, therefore, given by

$$\Delta N=N(\omega^2)-N_0(\omega^2)$$

$$=-\left(\frac{1}{\pi}\right)\mathrm{Im}\left(\frac{d}{d\omega^2}[\ln|\underline{I}+\underline{G}^0(z)\underline{P}(\omega^2)|\,]\right)\ . \tag{10}$$

For a crystal containing a single defect, the Green's function and perturbation matrices are $\underline{g}(z)$ and $\underline{p}(z)$, respectively, lying in the subspace $3b\times 3b$, $b$ being the total number of atoms disturbed by a single defect including the impurity itself. Hence, one can write Eq. (10) as

$$\Delta N=-\left(\frac{1}{\pi}\right)\mathrm{Im}\frac{d}{d\omega^2}\ln D(z)\ , \tag{11}$$

where $D(z)$ is the resonance denominator given by

$$D(z)=|\underline{I}+\underline{g}(z)\underline{p}(\omega^2)|\ .$$

For the case of a perturbation which possesses some symmetry, the resonance denominator of the $t$ matrix splits as

$$D(z)=\prod_\nu D_\nu(z)\ , \tag{12}$$

where

$$D_\nu(z)=|\underline{I}+\underline{g}_\nu(z)\underline{p}_\nu(\omega^2)|\ , \tag{13}$$

is the resonance denominator in the irreducible representation $\nu$, $\underline{g}_\nu(z)$ and $\underline{p}_\nu(\omega^2)$ are Green's function and perturbation matrices projected in the $\nu$th irreducible representation. The solutions of the equation

$$\mathrm{Re}\,D_\nu(z)=0\ , \tag{14}$$

give the resonance or the localized frequency depending on whether the frequency lies in the phonon spectrum or outside it.

Equation (10), which is true for any frequency lying in the phonon spectrum of the pure crystal, connects the scattering theory with the calculation of bulk properties of a dilute alloy. In this relation we obtain a change in the density of states relative to the entire crystal volume, so that if a finite concentration $cN$ ($N$ is the number of unit cells in the crystal) of noninteracting defects is present, we may merely multiply Eq. (10) by $cN$. Here $c$ denotes the fractional concentration of defects.

Thus the use of the symmetry-coordinates block diagonalizes the resonance denominator $D(z)$, and we may write

$$\Delta N(\omega^2)=-\sum_\nu \pi^{-1}\mathrm{Im}\frac{d}{d\omega^2}\ln D_\nu(z)=\sum_\nu \Delta N_\nu(\omega^2)\ , \tag{15}$$

where

$$\Delta N_\nu(\omega^2)=-\pi^{-1}l_\nu\,\mathrm{Im}\frac{d}{d\omega^2}\ln D_\nu(z)$$

$$=-\frac{l_\nu}{\pi}\mathrm{Im}\left(\frac{1}{D_\nu}\ \frac{dD_\nu(z)}{d\omega^2}\right)\ . \tag{16}$$

Here $\Delta N_\nu$ is the contribution from the $\nu$th irreduc-

ible representation and $l_\nu$ denotes the dimension of the $\nu$th irreducible representation.

The phonon phase shifts are defined by

$$\tan \delta_\nu = -\frac{\mathrm{Im}\, D_\nu(z)}{\mathrm{Re}\, D_\nu(z)} \ . \tag{17}$$

The introduction of these phase shifts immediately simplifies Eq. (16): The contribution to the change in the density of states produced by scattering in the irreducible representation $\nu$ becomes

$$\Delta N_\nu = \frac{l_\nu}{\pi}\frac{d\delta_\nu}{d\omega^2} \ . \tag{18}$$

This relation between the phase shift and the change in the density of states is true for any frequency lying in the frequency bands of the pure crystal.

### B. Lattice Specific Heat

The enhancement of the low-temperature vibrational specific heat by heavy impurity atoms per g mole ($N$ atoms) is given by

$$\Delta C_L(T) = \frac{\hbar^2}{4k_B T^2}\int_0^\infty \omega^2 \Delta N(\omega)\,\mathrm{csch}^2\frac{\hbar\omega}{2k_B T}\,d\omega \ , \tag{19}$$

where $\Delta N(\omega) = 2\omega \Delta N(\omega^2)$ and $k_B$ is the Boltzmann constant. The contribution from the $\nu$th representation in terms of phase shift is given by

$$\Delta C_L^\nu(T) = \frac{\hbar^2}{4k_B T^2}\int_0^\infty \omega^2\,\frac{l_\nu}{\pi}\,2\omega\frac{d\delta_\nu}{d\omega^2}\,\mathrm{csch}^2\frac{\hbar\omega}{2k_B T}\,d\omega \ . \tag{20}$$

Integrating once by parts, we have for the irreducible representations $\nu$

$$\Delta C_L^\nu(T) = -\frac{2k_B c N B^2}{\pi}\int_0^\infty \delta_\nu \omega\,\mathrm{csch}^2(B\omega) \times[1 - B\omega\coth(B\omega)]\,d\omega \ , \tag{21}$$

where $B = \hbar/2k_B T$.

### C. Defect Perturbation Model

The aluminum metal and its alloys with silver crystallize in fcc structures. If we assume a perturbation around an impurity where we consider a change in mass at the defect site and the change in the first-neighbor central-force constant of the de Launay type, the matrix $\underline{p}(\omega^2)$ is of $21\times21$ dimension. The irreducible representations occurring in this problem which exhibits a $O_h$ point-group symmetry are $F_{1u}$, $F_{2u}$, $F_{2g}$, $E_g$, and $A_{1g}$. The $t$ matrix in these irreducible representations for a diatomic fcc lattice has been obtained earlier by Agrawal.[13] The resonance denominators for a monatomic fcc lattice are given by

$$D_{A_{1g}}(z) = 1 + \lambda(g_1 + 2g_3 + 2g_4 + g_5 - g_6 - g_7 + g_9 - 2g_{10} + 4g_{12} + 2g_{13}) \ , \tag{22}$$

$$D_{E_g}(z) = 1 + \lambda(g_1 - g_3 - g_4 - g_5 - g_6 - g_7 + g_9 + g_{10} - 2g_{12} - g_{13}) \ , \tag{23}$$

$$D_{F_{2g}}(z) = 1 + \lambda(g_1 - g_5 + g_6 - g_7 + g_9) \ , \tag{24}$$

$$D_{F_{2u}}(z) = 1 + \lambda(g_1 - g_3 - g_4 + g_7 - g_9 - g_{10} + g_{12}) \ , \tag{25}$$

and

$$D_{F_{1u}}(z) = 1 - \epsilon\omega^2 g_1 + \tfrac{1}{2}\lambda(8x_1 - x_2 + x_3) + \tfrac{1}{2}\lambda\epsilon\omega^2[g_1(x_2 - x_3) - 8x_1(g_2 + g_4)] \ , \tag{26}$$

where $x_1$, $x_2$, and $x_3$ are the various combinations of Green's functions and are given by

$$x_1 = g_1 - g_2 + g_4 \ ,$$

$$x_2 = -g_1 + 8g_2 - 2g_3 - g_5 - g_6 - g_7 + g_9 - 2g_{10} + 2g_{12} \ ,$$

and

$$x_3 = g_1 + 10g_4 - g_5 - g_6 + g_7 - g_9 - 2g_{12} - 2g_{13} \ .$$

Here $\lambda$ is the change in the mass-reduced nearest-neighbor central-force constant and $\epsilon = (M' - M)/M$ is the change in mass at the impurity site ($M$ and $M'$ denote the masses of the host and impurity atom, respectively).

In case we define an effective force constant $\eta$ in the framework of nearest-neighbor rigid-ion model for the crystal lattice, the resonance denominator in the $F_{1u}$ irreducible representation can be simplified as[14]

$$D_{F_{1u}}(z) = \left(1 + \frac{\lambda}{\eta}\right)(1 - \epsilon\omega^2 g_1) + \frac{3\lambda}{\eta}(1 + \epsilon)\frac{\omega^2}{Z\eta}(1 + \omega^2 g_1) \ , \tag{27}$$

where $Z$ is the number of nearest neighbors of a lattice site and is equal to 12 for aluminum.

The various Green's functions for $\mu = 1$–$13$ are given by

$$g_\mu(\vec{R}_m - \vec{R}_n) = \frac{1}{N}\sum_{s=1}^{3}\sum_{\vec{k}}\frac{e^{i\vec{k}\cdot\vec{R}_{mn}}}{\omega_{\vec{k},s}^2 - z} \ , \tag{28}$$

where the summation is taken over all the wave vectors lying in the first Brillouin zone and $\vec{R}_{mn} = \vec{R}_m - \vec{R}_n$ is the difference in the lattice vectors of the two sites located at $\vec{R}_m$ and $\vec{R}_n$. The thirteen components of the Green's function are given in Table I.

## III. NUMERICAL COMPUTATIONS AND RESULTS

### A. Lattice Dynamics of Aluminum

Aluminum is a trivalent metal and possesses monatomic face-centered cubic structure. The same is true for its dilute alloys with silver. It has been observed that the resistance to shear in these metals arises due to Coulomb interaction between the ions and conduction electrons and the

TABLE I Different matrix elements of the Green's function.

| Green's function | Component |
|---|---|
| $g_1$ | $g_{xx}(0, 0, 0)$ |
| $g_2$ | $g_{xx}(\frac{1}{2}, \frac{1}{2}, 0)$ |
| $g_3$ | $g_{xx}(0, \frac{1}{2}, \frac{1}{2})$ |
| $g_4$ | $g_{xy}(-\frac{1}{2}, -\frac{1}{2}, 0)$ |
| $g_5$ | $g_{xx}(0, 1, 0)$ |
| $g_6$ | $g_{xx}(1, 0, 0)$ |
| $g_7$ | $g_{xx}(1, 1, 0)$ |
| $g_8$ | $g_{xx}(0, 1, 1)$ |
| $g_9$ | $g_{xy}(-1, -1, 0)$ |
| $g_{10}$ | $g_{xx}(1, \frac{1}{2}, \frac{1}{2})$ |
| $g_{11}$ | $g_{xx}(\frac{1}{2}, \frac{1}{2}, 1)$ |
| $g_{12}$ | $g_{xy}(-1, -\frac{1}{2}, \frac{1}{2})$ |
| $g_{13}$ | $g_{xy}(-\frac{1}{2}, -\frac{1}{2}, 1)$ |

short-range interaction between the ions. An eight-neighbor force-constant model has been utilized by Gilat and Nicklow[15] to explain the dispersion curves obtained by Stedman and Nilsson[16] by performing inelastic-neutron-scattering experiments. Gilat and Nicklow have not considered the influence of free electrons on the ionic motion. In the present work we have discussed the lattice dynamics of pure aluminum at 80 °K in Krebs's model,[17] where one takes into account the effects of electrons on the motion of ions via screened Coulomb interaction between the ions. We consider the ion-ion interactions of central type up to three neighbors. The values of the elastic constants used are $c_{11} = 11.373 \times 10^{11}$ dyn cm$^{-2}$, $c_{12} = 6.191 \times 10^{11}$ dyn cm$^{-2}$, and $c_{44} = 3.128 \times 10^{11}$ dyn cm$^{-2}$. The value of the lattice constant is 4.04 Å. The values of the effective charge $e^*$ and the Bohm–Pines parameter $\beta$ are taken to be 3 and 0.500, respectively. The wave-vector dependence of the screening parameter has been considered in terms of the factor $f(t)$ given by

$$f(t) = \frac{1}{2} + \frac{1-t^2}{4t} \ln\left|\frac{1+t}{1-t}\right| , \tag{29}$$

where $t = k/2k_F$ and $k_F$ is the radius of the Fermi surface in the wave-vector space. A similar calculation has been done by Shukla and Dayal[18] after approximating the factor $f(t)$ by unity and using a lower value of $\beta$, i.e., 0.353. The frequencies and the polarization vectors are determined by diagonalizing the $3 \times 3$ dynamical matrix by Jacobi's method. A grid of 8000 points in the first Brillouin zone was seen to give reasonably good results. The results obtained for the three symmetry directions [$(\zeta,0,0)$, $(\zeta,\zeta,0)$, and $(\zeta,\zeta,\zeta)$] are presented in Fig. 1. Here $\zeta$ is the reduced wave vector equal to $k/k_{max}$. The results have been compared with the experimental results of Stedman and Nilsson.[16] A very good agreement is seen between the theory and the experiment except for some small discrepancies near the Brillouin zone. The density of states has been shown in Fig. 2.

### B. Green's Functions

The Green's functions were computed by employing a staggered-bin averaging method. The real and imaginary parts of a Green's function may be written

$$g_\mu(\omega^2) = \frac{1}{N} \sum_{\vec{k}} \sum_s \frac{j_\mu(\vec{k}|s)}{\omega^2_{\vec{k},s} - z}$$

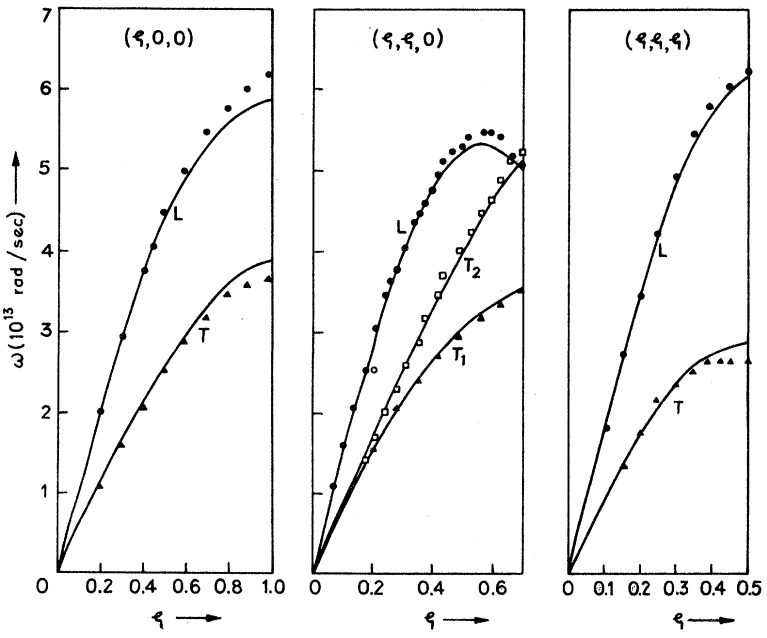


FIG. 1. Dispersion curves for pure aluminum in the three symmetry directions $(\zeta, 0, 0)$, $(\zeta, \zeta, 0)$, and $(\zeta, \zeta, \zeta)$. Points denote experimental results and full curves denote the results of the present calculations. The longitudinal and transverse branches are represented by $L$ and $T$, respectively ($T_1$ and $T_2$ denote the two transverse branches).

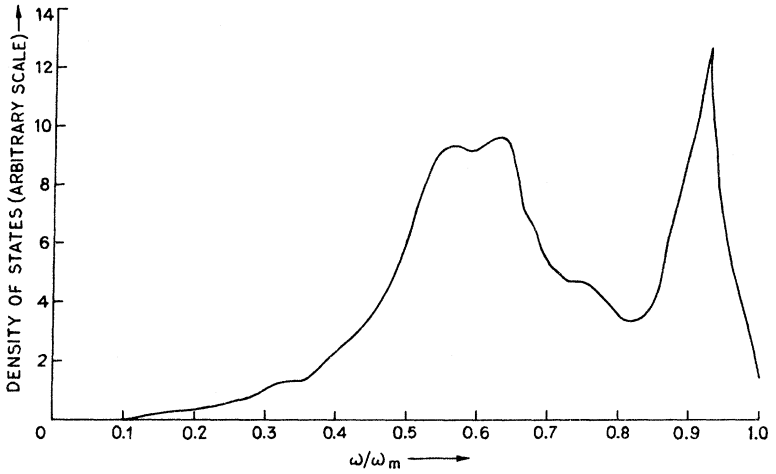


FIG. 2. Density of vibrational states in pure Al.

$$= \frac{1}{N} \mathrm{p} \sum_{\vec{k}} \sum_{s} \frac{j_\mu(\vec{k}|s)}{\omega^2_{\vec{k},s} - \omega^2} + i\pi \frac{1}{N} \sum_{\vec{k}} \sum_{s} j_\mu(\vec{k}|s)\delta(\omega^2_{\vec{k},s} - \omega^2) , \quad (30)$$

where $j_\mu(\vec{k}|s)$ is a real quantity obtained after summing a number of equivalent Green's functions. The imaginary part is calculated first and a histogram is obtained by expressing it as

$$\mathrm{Re}G(\omega^2) = \int_0^{\omega_m} d\omega' \frac{S(\omega') - S(\omega)}{\omega'^2 - \omega^2} - \frac{S(\omega)}{2\omega} \ln \frac{\omega_m + \omega}{\omega_m - \omega} , \quad (31)$$

where $S(\omega) = \sum_{\vec{k}} \sum_s j(\vec{k}|s)\, \delta(\omega_{\vec{k},s} - \omega)$ and $\omega_m$ is the maximum frequency. In order to carry out integrations the real part of the total frequency range was divided into 60 equal bins. The histogram for each Green's function was computed in the center of each bin. Spurious fluctuations in the Green's functions were reduced by choosing a finite bin width, i.e., 0.25 in the units of bin width.

### C. Specific Heat

The contribution to the specific heat has been calculated using Eq. (21) by varying the central force constant-change parameter $\lambda$ for the two concentrations of silver in aluminum. The results for three values of $\lambda$, i.e., $\lambda = -0.45\times10^{26}$, $-0.50\times10^{26}$, and $-0.55\times10^{26}$ sec$^{-2}$, are presented in Figs. 3 and 4. The results of the mass defect theory ($\lambda = 0$) are also shown in these figures. Reasonably good results are obtained for $\lambda = -0.50\times10^{26}$ sec$^{-2}$. We find from the figures that the use of a smaller value for the force constant between the impurity and the host lattice gives larger contribution to the specific heat, whereas the opposite is the case with a greater impurity host-ion interaction. The result is in agreement with that obtained earlier by one of the authors[19] using a simple expression for the specific heat in a scalar

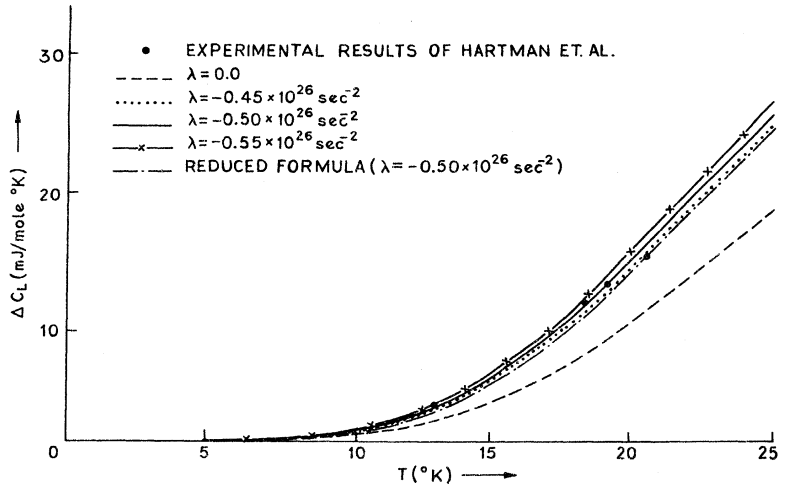


FIG. 3. Enhanced lattice specific heat in $Al_{99.50}Ag_{0.50}$ alloy.

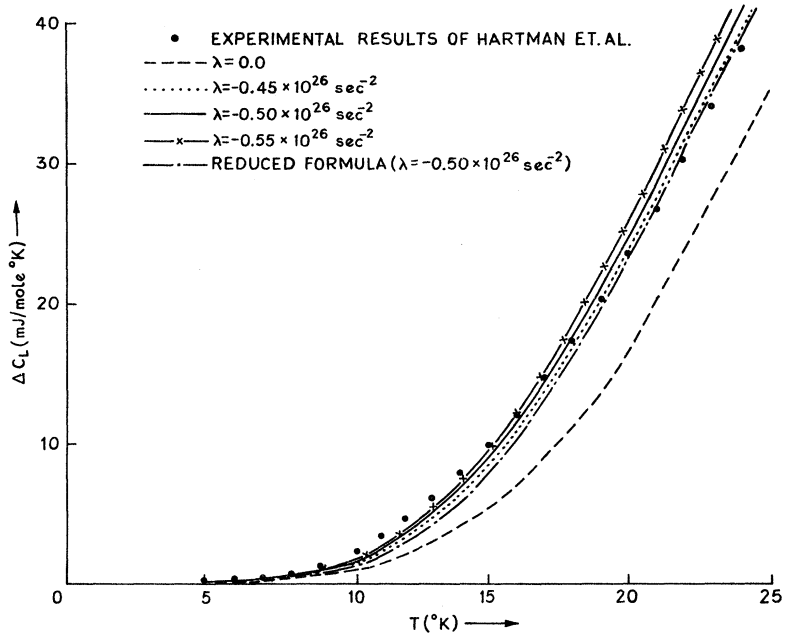


FIG. 4. Enhanced lattice specific heat in $Al_{99.05}Ag_{0.95}$ alloy.

model of the lattice.

The real part of the resonance denominators for $\lambda = -0.50\times10^{26}\,\mathrm{sec}^{-2}$ and for $F_{1u}$-symmetry motion has been plotted in Fig. 5. The $F_{1u}$-mode resonance frequency $\omega_r$ lies at 84 $\mathrm{cm}^{-1}$ for $\lambda = -0.50\times10^{26}$ $\mathrm{sec}^{-2}$. For an isotopic defect this resonance mode appears at 94 $\mathrm{cm}^{-1}$ ($\omega_r/\omega_m = 0.29$) which is in very good agreement with the values obtained by Hartmann *et al.* ($\omega_r/\omega_m = 0.28$). Another solution of Eq. (14) appears at 177 $\mathrm{cm}^{-1}$ which is seen to be an antiresonance mode.

The phase shift in the $F_{1u}$ irreducible representations has been plotted in Fig. 6. The phase shift is seen to be equal to $\frac{1}{2}\pi$ for both the resonance and antiresonance modes appearing at 84 and 177 $\mathrm{cm}^{-1}$, respectively. The contribution of the antiresonance mode is found to be negative in accordance with the expected behavior that the density of states should decrease at this frequency. However, its contribution is insignificant at very low temperatures.

In order to see the contributions of the various irreducible representations we have also shown phase shifts for $A_{1g}$ and $E_g$ modes in Fig. 7 and for $F_{2g}$ and $F_{2u}$ modes in Fig. 8. It may be noted that the contributions of these four representations ($A_{1g}$, $E_g$, $F_{2g}$, and $F_{2u}$) are much smaller than the $F_{1u}$ mode. In fact, the contributions of $A_{1g}$, $E_g$, $F_{2g}$, and $F_{2u}$ to the specific heat at 6 °K are 3.5, 2.5, −0.2, and 10.2%., respectively, while the contribution of the $F_{1u}$ modes at this temperature

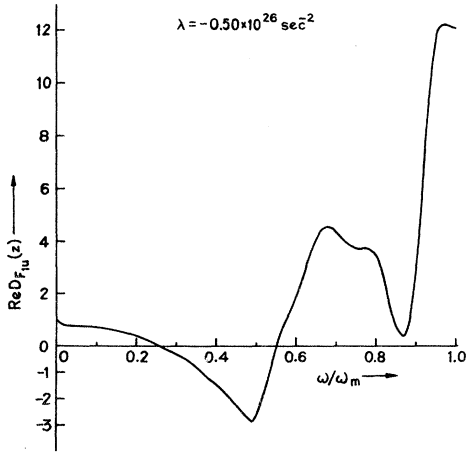


FIG. 5. Real part of determinant for $F_{1u}$ symmetry modes.

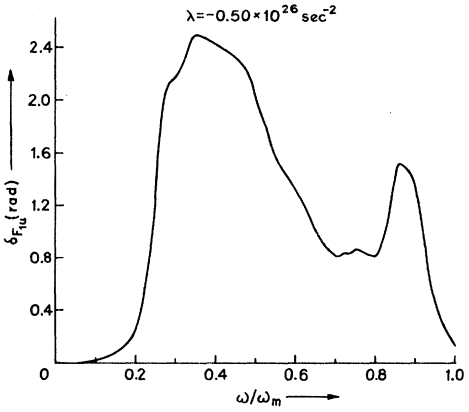


FIG. 6. Phase shifts for $F_{1u}$ symmetry modes.

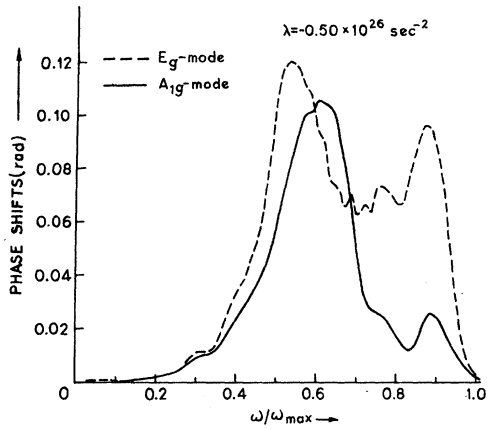


FIG. 7. Phase shifts for $E_g$ and $A_{1g}$ symmetry modes.

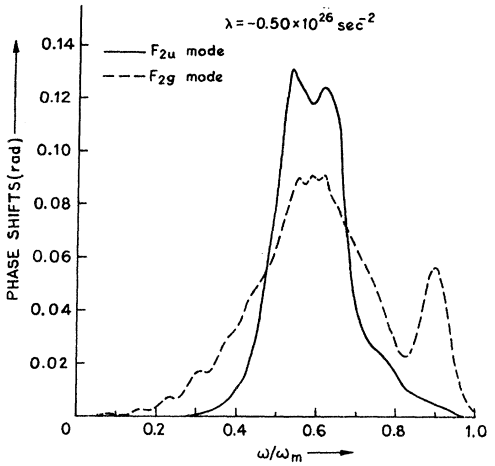


FIG. 8. Phase shifts for $F_{2u}$ and $F_{2g}$ symmetry modes.

is 84%. At 24 °K the contribution of each of the $A_{1g}$, $E_g$, $F_{2g}$, and $F_{2u}$ symmetry modes is within 1% and the contribution of the $F_{1u}$ modes is about 98%.

### D. Effective Force Constant

Calculations have also been made for the contribution of $F_{1u}$ irreducible representation by using $D_{F_{1u}}(z)$ given by Eq. (27) which has been obtained by defining an effective nearest-neighbor central force constant $\eta$ for the pure lattice. This effective force constant can be evaluated by solving Eq. (27) after using $\lambda = -0.50\times10^{26}$ sec$^{-2}$ and the resonance frequency at 84 cm$^{-1}$. The results obtained in this approximation have been shown in Figs. 3 and 4 for the two concentrations. It is observed that these approximate values are in general smaller than the actual values obtained in a realistic manner [using Eq. (26)] by about 12% at 15 °K and about 5% at 24 °K for the two alloys of aluminum.

The value of the effective force constant $\eta$ comes out to be $1.521\times10^4$ g/sec$^2$ which is very near to the value of the first-neighbor central-force constant, i.e., $1.609\times10^4$ g/sec$^2$ used in the calculation of lattice dynamics of aluminum.

## IV. DISCUSSIONS AND CONCLUSIONS

We have made a detailed study of the effects of force constant changes on the lattice specific heat of dilute Al : Ag alloys having fcc structures. Numerical calculations have been performed for the two very dilute alloys containing 0.5 and 0.95 at.% of Ag as impurity atoms. A decrease in the impurity-host interaction enhances the contribution to the specific heat and vice versa. This qualitative conclusion is in agreement with the result of an expression obtained earlier in an analytical manner for a scalar model of crystal lattice by one of the authors. The calculated results compare very well with the experimental ones. The enhancement in specific heat arises mainly due to $F_{1u}$ symmetry resonance modes and the contribution increases with an increase in the temperature of the solid, e.g., the contribution is 84% at 6 °K and becomes 98% at 24 °K. The effective central force constant for the pure lattice evaluated by using the resonance frequency is in very good agreement with that obtained on the basis of a force constant model and is, therefore, reliable to perform involved computations. The results obtained in this approximation are smaller only by 12% at low temperatures and 5% at higher temperatures. At still higher temperatures the difference in the two calculations may be insignificant.

## ACKNOWLEDGMENTS

The authors are grateful to the Computer Centres at I.I.T., Kanpur and Delhi School of Economics, Delhi University, for providing the facilities to work on the IBM 7044 and IBM 360/44 computers. We are also thankful to the Council of Scientific and Industrial Research, New Delhi for financial assistance.

[1]A. A. Maradudin, Rep. Prog. Phys. **28**, 332 (1965).
[2]A. A. Maradudin, in *Solid State Physics*, edited by F. Seitz and D. Turnbull (Academic, New York, 1966), Vol. 18, p. 273.
[3]I. M. Lifshitz, Rep. Prog. Phys. **29**, 277 (1966).
[4]R. M. Cunningham, L. D. Muhlestein, W. W. Shaw, and C. W. Tompson, Phys. Rev. B **2**, 4864 (1970).
[5]E. C. Svensson and W. A. Kamitkahara, Can. J. Phys. **49**, 2291 (1971).
[6]K. M. Kesharwani and Bal K. Agrawal, Phys. Rev. B **6**, 2178 (1972).
[7]G. W. Lehman and R. E. De Wames, Phys. Rev. **131**, 1008 (1963).
[8]Yu. M. Kagan and Ya. A. Iosilevskii, Zh. Eksp. Teor. Fiz. **45**, 819 (1963) [Sov. Phys.-JETP **18**, 562 (1964)].

[9]G. W. Lehman, J. A. Cape, R. E. De Wames, and D. H. Leslie, Bull. Am. Phys. Soc. **2,** 251 (1964); J. A. Cape, G. W. Lehman,W. V. Johnston, and R. E. De Wames, Phys. Rev. Lett. **16,** 892 (1962).
[10]G. Kh. Panova and B. N. Samoilov, Zh. Eksp. Teor. Fiz. **49,** 456 (1965) [Sov. Phys.-JETP **22,** 327 (1966)].
[11]H. V. Culbert and R. O. Huebener, Phys. Lett. **24,** 530 (1967).
[12]W. M. Hartmann, H. V. Culbert, and R. P. Huebener, Phys. Rev. B **1,** 1486 (1970).
[13]Bal Krishna Agrawal, Phys. Rev. **186,** 712 (1969).
[14]Bal K. Agrawal and P. N. Ram, Phys. Rev. B **4,** 2774 (1971).
[15]G. Gilat and R. M. Nicklow, Phys. Rev. **143,** 487 (1966).
[16]R. Stedman and G. Nilsson, *Inelastic Scattering of Neutrons in Solids and Liquids* (International Atomic Energy Agency, Vienna, 1965), Vol. I, p. 211.
[17]K. Krebs, Phys. Rev. 138, A143 (1965).
[18]M. M. Shukla and B. Dayal, Phys. Status Solidi **16,** 513 (1966).
[19]Bal K. Agrawal, J. Phys. C **2,** 252 (1969).

PHYSICAL REVIEW B VOLUME 7, NUMBER 6 15 MARCH 1973

# Pseudopotential Calculation of the Third-Order Elastic Constants of Copper and Silver*

J. F. Thomas, Jr.†
*Physics Department, University of Virginia, Charlottesville, Virginia 22901*
(Received 28 August 1972)

The third-order elastic constants of copper and silver have been calculated by the method of homogeneous deformation from a total energy expression consisting of four terms: a free-electron energy, an electrostatic energy, a band-structure energy, and an ion-core overlap energy. The band-structure energy has been expressed in terms of a local pseudopotential. The overlap energy has been approximated by a Born–Mayer potential. The total-energy expression includes five adjustable parameters which have been chosen to fit the binding energy, lattice spacing, and three second-order elastic constants to experiment. The ion-core repulsive energy makes the dominant contribution to the third-order elastic constants. The other contributions are not negligible but tend to cancel. The calculated third-order elastic constants of copper and silver are in good agreement with low-temperature experimental values. An attempt to apply the five-parameter fitting procedure to gold was unsuccessful.

## I. INTRODUCTION

Pseudopotential theory has been remarkably successful in the calculation of structural properties, such as elastic constants and phonon spectra of simple (*sp*-bonded) metals. Unfortunately, the situation is quite the opposite for the transition metals. There is now no distinct approach of comparable power applicable to this important class of materials. This is true, also, for the noble metals copper, silver, and gold which, in many respects, form a link between the simple metals and the transition series.

Several years ago, Harrison[1] proposed a scheme by which the pseudopotential formalism could be applied to transition metals. The key result was that hybridization between the *d* bands and conduction band could be included in a weak pseudopotential. Perturbation theory could then be used in the usual way to obtain an analytical expression for the lattice energy as a function of the ion positions.[2] Harrison's approach has been developed by Moriarty.[3–5] He recently completed numerical calculations of the total energy of the noble metals and applied the results to predict crystal structure and calculate phonon spectra with moderate, yet encouraging, success.[5]

The purpose of this work is to calculate the third-order elastic (TOE) constants of the noble metals. Interest in TOE constants, which measure the anharmonic part of the interatomic potentials, has centered on information which can be obtained regarding the lattice energy or interatomic potential. For example, by symmetry, there are six TOE constants for a cubic crystal. Experimental values of these parameters for the noble metals,[6–10] including some measurements at low temperature,[8–10] are available to fit or verify a theoretical interatomic potential.

We have calculated the TOE constants by the method of homogeneous deformation. The total-energy expression used in the calculation is based upon the work of Harrison[1] and Moriarty.[5] However, we have made several simplifying assumptions, including the use of a local-empirical pseudopotential, to keep the calculation of the required energy derivatives tractable. To partially compensate, we have included five adjustable parameters in the total-energy expression. These have been chosen to fit the binding energy, lattice spacing, and three second-order elastic (SOE) constants to their experimental values. The total-energy expression consists of four terms: the free-electron energy $U_{fe}$, the electrostatic energy $U_{es}$, the band-structure energy $U_{bs}$, and the overlap energy $U_{ol}$. The energy term $U_{ol}$, which measures the exchange interaction between neighboring ion cores, has been approximated in terms of the